Hindawi
Mathematical Problems in Engineering
Volume 2017, Article ID 9840172, 10 pages
https://doi.org/10.1155/2017/9840172

Research Article

Radar Communication Integrated Waveform Design Based on OFDM and Circular Shift Sequence

Cong Li, Weimin Bao, Luping Xu, Hua Zhang, and Ziyang Huang

School of Aerospace Science and Technology, Xidian University, Xi'an 710126, China

Correspondence should be addressed to Luping Xu; xlpingedu@126.com

Received 10 February 2017; Revised 22 May 2017; Accepted 25 May 2017; Published 13 July 2017

Academic Editor: Alessandro Lo Schiavo

Based on the orthogonal frequency division multiplexing (OFDM) technique, an intelligent waveform is designed, which is suitable for simultaneously performing data transmission and radar sensing. In view of the inherent high peak-to-mean envelope power ratio (PMERP) and poor peak-to-side-lobe ratio (PSLR) problems in the OFDM based radar and communication (RadCom) waveform design, we propose two technologies to deal with that. To be specific, we adopt Gray code technology to reduce the PMERP and simultaneously choose an optimal cyclic sequence to improve the PSLR of RadCom waveform. In our method, the optimal cyclic sequence is dynamically generated to continuously provide the best waveform according to the change of communication data. In addition, to meet the requirements of different radar detection tasks, two simple methods are utilized to adjust the bandwidth of RadCom waveform. To verify the advantages of the designed waveform, we conduct several simulation experiments to compare with some existing RadCom waveforms. The results show that our designed RadCom waveform can simultaneously achieve lower PMERP and higher PSLR. In addition, our designed RadCom waveform has a thumbtack type fuzzy function and shows the good ability to do multitarget detection.

1. Introduction

The demand for radio-frequency bandwidth is rising, driven by the increasing requirements of consumers for high quality communications and radar detection ability. By using a joint radio-frequency hardware platform for communications and radar applications [1–9], the occupied spectrum can be used very efficiently, which helps to partially overcome the limited availability of spectral resources. There is a large area of applications which possibly benefit from the availability of radar and communication (RadCom) systems, such as intelligent transportation network, radar ad hoc network, and deep space network. Intelligent transportation system [10], for instance, require intelligent vehicles to have the ability to work in an autonomous manner to sense the driving environment and provide unique safety features and intelligent traffic routing. The main challenge in RadCom development lies in finding suitable waveforms that can be simultaneously employed for information transmission and radar sensing.

For communications, data rate and bit error rate are the most important parameters. In order to achieve better communications performance in terms of data rate, continuous waveforms have to be applied. As for the radar function, dynamic range and resolution are critical requirements for object detection. To guarantee the high dynamic range of the measurements, radar waveform designers aim at creating waveforms with optimum autocorrelation properties. A typical continuous waveform with good autocorrelation properties is single-carrier based RadCom waveform combined with code-domain (spread spectrum) scheme [11–14]. In addition, advanced concepts based on multicarrier communication waveforms, also often denoted as orthogonal frequency division multiplexing (OFDM), are proposed [8, 15–18]. Compared with single-carrier waveform, OFDM waveforms offer a number of advantages, such as the availability of processing gain at the receiver, high spectrum efficiency, and good antimultipath performance. However, OFDM based RadCom waveform design also faces some challenging problems, such as a relatively high PMERP and

undesirable autocorrelation properties or peak-to-side-lobe ratio (PSLR).

To reduce the PMERP of RadCom waveform, one popular method is to design different subcarrier complex weights [15, 17] and the other method is utilizing phase code technique [19, 20]. These two methods can also be adopted to improve the PSLR of RadCom waveform. Nevertheless, a lower PMERP and higher PSLR of RadCom waveform cannot be achieved simultaneously by using either of these two methods. The reason may be that a lower PMERP always means a poor side lobe level (SLL) suppression when subcarrier complex weight or phase code technique is adopted to reduce the PMERP. In [15], the authors use direct spread spectrum sequence (DSSS) to improve the PSLR of RadCom waveform but ignore the PMERP problem. In [17], chaos-based phase code sequence is utilized to get a good autocorrelation property and the PMERP is suppressed by adding window function. But these two issues are processed separately; in other words, the effects of chaos-based sequence on the PMERP and window function on the PSLR are not taken into account. To address these issues, we present a new designed OFDM based RadCom waveform. For the PMERP problem, a Gray code coding technique is adopted to reduce the PMERP. To improve the PSLR of RadCom waveform, a cyclic shift sequence is proposed, which has no effect on the PMERP but plays an important role in the SLL suppression. Thus, in this paper, a lower PMERP and desired PSLR can be achieved simultaneously by adopting the Gray code technology and choosing an optimal cyclic shift sequence. In addition, taking into account the different detection precision requirements of various radar tasks, two convenient ways are adopted to dynamically adjust the bandwidth of RadCom waveform.

The rest of the paper is organized as follows. The RadCom signal model is presented in Section 2 and the structure of RadCom waveform is described in Section 3. Then the performance analysis and simulation results analysis of RadCom waveform follow in Sections 4 and 5. Finally, conclusions are drawn in Section 6.

2. RadCom Signal Model

Multicarrier Phase Coded (MCPC) signals featured by low SLL, high spectrum efficiency, and an ideal pin-type ambiguity function have been widely adopted in radar waveform design. The complex envelope of a single MCPC waveform is given by [20].

$$s_R(t) = \sum_{n=0}^{N_c-1}\sum_{m=0}^{M-1} w_n p_{m,n} u\left[t-(m-1)t_b\right]\exp\left(j2\pi f_n t\right), \quad 0 \le t < Mt_b,\ 0 \le n < N_c, \tag{1}$$

where w_n is the complex weight of the nth subcarrier, satisfying $\sum_{n=0}^{N_c-1}|w_n|^2 = 1$, $p_{m,n}$ is the mth element of the sequence which modulates the nth subcarrier, $u(t)$ is the gate function, t_b is subpulse width, $f_n = n \cdot \Delta f$ is the nth subcarrier, $\Delta f = 1/t_b$ is frequency space, N_c is the number of subcarriers, and M is the number of OFDM symbols. Based on the MCPC technology, especially OFDM technology, two RadCom waveforms are presented [15, 17], which can be written as

$$s_{RC}(t) = \sum_{n=0}^{N_c-1}\sum_{m=0}^{M-1} w_n b_{m,n} p_{m,n} u\left[t-(m-1)t_b\right]\exp\left(j2\pi f_n t\right), \quad 0 \le t < Mt_b,\ 0 \le n < N_c, \tag{2}$$

where $b_{m,n}$ is communication data within a subpulse, $w_n = A_n e^{j\varphi_n}$ is the complex weight, A_n is the amplitude, and φ_n is the phase. w_n is usually used for adjusting the PMERP of RadCom waveform. $p_{m,n}$ is the phase sequence, which greatly affects the performance of RadCom waveform and different RadCom waveform designing approaches focus on the phase sequence designs. In literature [15], $p_{m,n}$ is designed as direct spread spectrum sequence, while, in [17], $p_{m,n}$ is designed as chaos-based phase code sequence. Similar to these two methods, in this paper, $p_{m,n}$ is designed as a circular shift sequence within the subpulse t_b. A time-domain circular shift for any arbitrary t_m of the mth pulse of RadCom is represented as

$$\begin{aligned} s_{RCm}(t) &= \sum_{n=0}^{N_c-1} w_n b_{m,n} p_{m,n} \exp\left[j2\pi f_n (t-t_m) \bmod t_b\right] \\ &= \sum_{n=0}^{N_c-1} w_n b_{m,n} p_{m,n} \exp\left(j2\pi f_n t\right)\exp\left(-j2\pi\frac{nt_m}{t_b}\right) \\ &= \sum_{n=0}^{N_c-1} w_n b_{m,n} a_{m,n} \exp\left(j2\pi f_n t\right), \end{aligned} \tag{3}$$

where $a_{m,n} = p_{m,n}\exp(-j2\pi n t_m/t_b)$. Then the proposed RadCom waveform can be finally expressed as

$$\begin{aligned} S_{RC}(t) &= \sum_{m=1}^{M} s_{RCm}\left[t-(m-1)t_b\right] \\ &= \sum_{n=0}^{N_c-1}\sum_{m=1}^{M} w_n b_{m,n} a_{m,n} u\left[t-(m-1)t_b\right]\exp\left(j2\pi f_n t\right), \\ &\qquad 0 \le t < Mt_b,\ 0 \le n < N_c. \end{aligned} \tag{4}$$

As we all know, OFDM signal is sensitive to Doppler spread and some Doppler processing methods are proposed [21, 22]. In this paper, we assume that the Doppler has been complemented and do not consider the impact of Doppler. Thus, if an OFDM based RadCom signal is reflected at L objects, the received signal can be described as

$$\begin{aligned} S_r(t) &= \sum_{l=0}^{L-1} S_{RC}(t-\tau_l) \\ &= \sum_{l=0}^{L-1}\sum_{n=0}^{N_c-1}\sum_{m=1}^{M} w_n b_{m,n} a_{m,n} u\left[t-(m-1)t_b-\tau_l\right] \\ &\quad \cdot e^{j2\pi f_n (t-\tau_l)}, \end{aligned} \tag{5}$$

where $\tau_l = 2R_l/c$; R_l is the distance from the lth target to the radar. For a radar signal, the high resolution range profile (HRRP) can be achieved by pulse compression. In this paper, the pulse compression is realized through a time-domain matched filter. The impulse response of time-domain matched filter is given as

$$h(t) = S_{RC}{}^{*}(-t), \tag{6}$$

where $(\,)^{*}$ represents the complex conjugate. Then the matched filter output of RadCom echo is expressed as

$$y(t) = S_r(t) \otimes h(t) = \int_{-\infty}^{+\infty} S_r(\tau)\, S_{RC}{}^{*}(\tau - t)\, dt, \tag{7}$$

where $\otimes$ is convolution computation. Time-domain convolution takes a large amount of calculation. In order to reduce calculation amount, the convolution is realized by an FFT in frequency domain. Assuming the Fourier transform of $S_{RC}(t)$ is $S_{RC}(f)$, then the Fourier transform of $S_r(t)$ and $y(t)$ can be achieved, respectively, as

$$S_r(f) = \sum_{l=0}^{L-1} S_{RC}(f)\, e^{-j2\pi f\tau_l}, \tag{8}$$

$$Y(f) = S_r(f)\, S_{RC}{}^{*}(f) = \sum_{l=0}^{L-1} \left|S_{RC}(f)\right|^2 \cdot e^{-j2\pi f\tau_l}. \tag{9}$$

Making an IFFT conversion for (9) will yield the HRRP.

$$s_{\mathrm{HRRP}}(t) = R_s(t) \otimes \sum_{l=0}^{L-1} \delta(t - \tau_l) = \sum_{l=0}^{L-1} R_s(t - \tau_l), \tag{10}$$

where $R_s(t)$ is an IFFT version of $|S_{RC}(f)|^2$ and also an autocorrelation function of $S_{RC}(t)$. Equation (10) denotes that in each inverse Fourier transform the signals obtain a total power gain of N^2, whereas noise, as a stochastic quantity, only experiences a power gain of N. Hence, the total processing gain G_p of proposed RadCom waveform is

$$G_p = N_c M. \tag{11}$$

3. Structure of RadCom Waveform

In order to better understand the structure of RadCom, an application scenario is illustrated in Figure 1. The RadCom signal (colored in blue) is transmitted from car 1 on the left. This signal transports communication information to a distant receiver, for example, car 2. At the same time, this RadCom signal is reflected from car 2 and car 3 (reflected signal depicted in red). The RadCom system receives the echoes of its own transmit signal and detects the presence of reflecting objects. For radar processing, it can be assumed that the transmitted signal is known at the radar receiver. For communication processing, the modulation type is perfectly known to the communication terminal. The whole process or structure of the RadCom waveform is shown in Figure 2.

As shown in Figure 2, the communication data is encoded by Gray code and then is sent to the mapping module. The

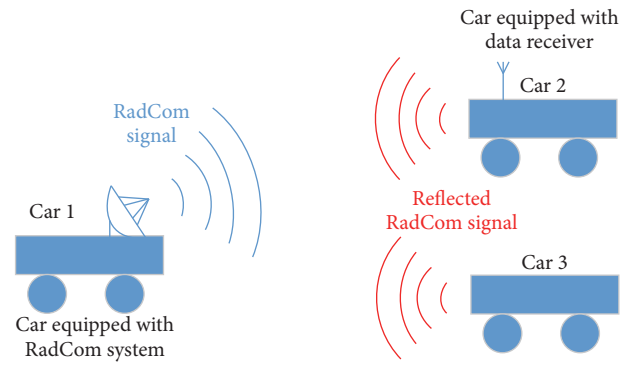

Figure 1: RadCom application scenario in the intelligent transportation system.

selecting and mapping modules are used for adjusting the bandwidth of RadCom waveform. Depending on the different requirements of RadCom systems, the communication data are mapped as different new sequences. Then the new sequences are sent to circular shift module and an optimal circular shift sequence is sought to maximize the autocorrelation performance of the RadCom system. Next, the IFFT module is utilized to form the OFDM signal. So far, the OFDM based RadCom baseband waveform has been formed. As shown in Figure 1, the radar transmitter and receiver are at one location and the communication receiver is at a different location. The communication terminal receives the signal transmitted by RadCom system and the demodulation process is an inverse process of the modulation process. In contrast, radar terminal receives the echo of a RadCom signal after being reflected by the target and finally gets the HRRP by pulse compression technology.

To adapt to the precision requirements of different radar detection tasks, the designed RadCom waveform needs to provide different bandwidth easily. In this paper, increasing the number of subcarriers N while keeping the frequency interval Δf constant is denoted as method 1. On the contrary, increasing the frequency interval Δf while keeping the number of subcarriers N constant is considered as method 2. The examples of enlarging the bandwidth twofold with these two methods are shown in Figure 3.

Figure 3(a) shows that the number of subcarriers is changed from N to $2N$ and the communication data $b_1, b_2, \ldots, b_{2N}$ are embedded into all of the subcarriers. This means that the bandwidth of radar waveform increases twofold, and so does the communication rate. The shortcomings of this method lie in that increasing the subcarriers leads to a higher PMERP and also increases the computation of searching for the best cyclic shift. From Figure 3(b), it can be seen that the communication data sequence $b_1, b_2, \ldots, b_N$ is mapped as $b_1, 0, b_2, \ldots, b_{N/2}, 0, b_{N/2+1}, \ldots, 0, b_N$ which denotes that the frequency interval is enlarged twofold and the communication data rate is constant. A bigger frequency interval usually means a higher Doppler tolerance and a more stronger immunity to phase noise [23], which is useful for the subsequent signal processing. In short, method 1 obtains a high-speed data communication at the cost of a

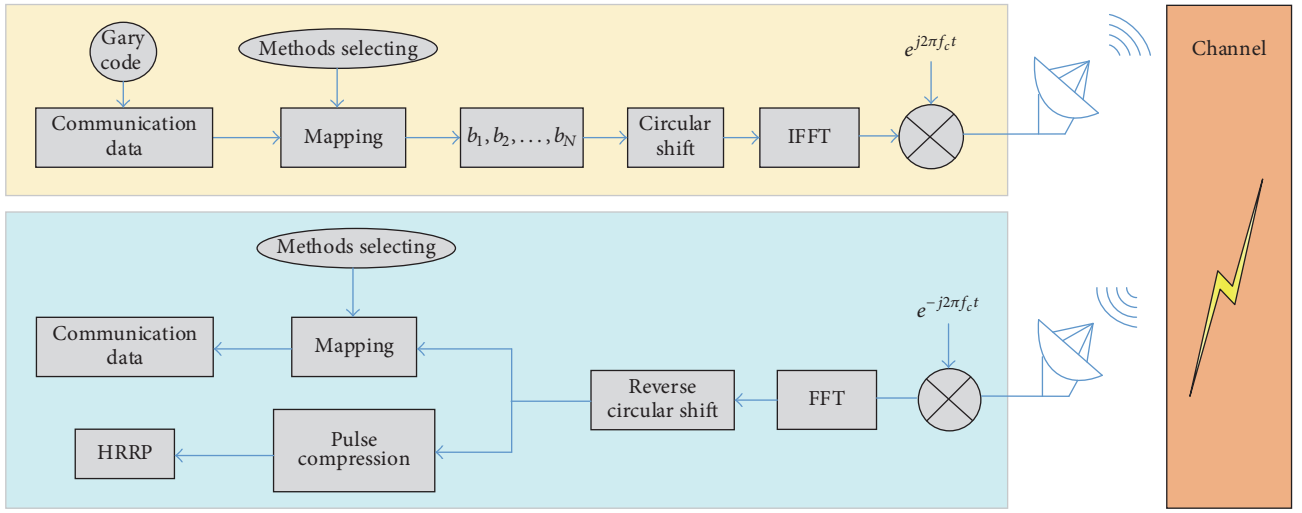

Figure 2: Structure of RadCom waveform.

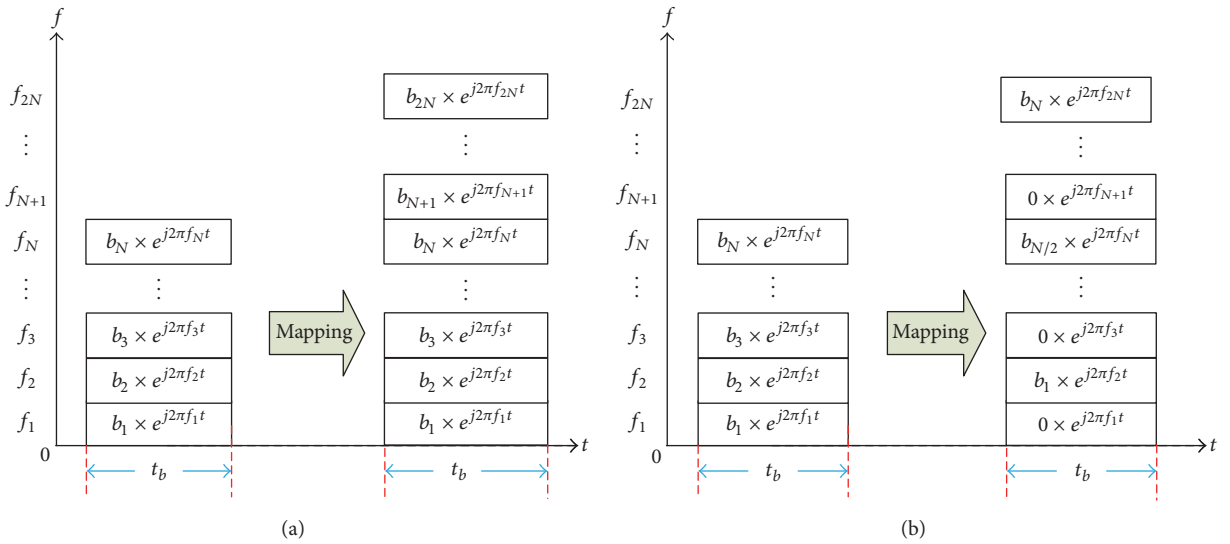

Figure 3: Expanding the bandwidth of RadCom waveform by two methods. (a) Increasing the subcarrier numbers; (b) increasing the frequency interval.

high complexity of reducing the PMERP and PSLR, while method 2 is suitable for a low bit-rate communication and low requirement of the computational complexity of RadCom system.

4. Theoretical Performance Analysis of RadCom Waveform

4.1. Theoretical Analysis of PMERP. Large amplitude fluctuation is a major drawback of OFDM based RadCom waveform and many methods have been proposed to reduce the PMERP [19, 20, 24]. For the mth subpulse $s_m(t)$, the PMERP is denoted as

$$\text{PMERP} = \frac{\max\left(\left|s_m(t)\right|^2\right)}{(1/t_b)\int_0^{t_b}\left|s_m(t)\right|^2 dt}. \tag{12}$$

For the complex RadCom signal $s_m(t)$, it can be shown by straightforward calculation that

$$\begin{aligned}\left|s_m(t)\right|^2 &= \sum_{n=0}^{N-1}\sum_{l=0}^{N-1}(w_n b_n a_n)^* \cdot (w_l b_l a_l)\exp\left[j2\pi\left(f_l - f_n\right)t\right] \\ &= \sum_{n=0}^{N-1}\left|w_n b_n a_n\right|^2 + 2\text{Re}\left\{\sum_{k=1}^{N-1} m_k \exp\left(j2\pi k\Delta f t\right)\right\},\end{aligned} \tag{13}$$

where $m_k = \sum_{n=0}^{N-k-1}(w_n b_n a_n)^* \cdot (w_{n+k} b_{n+k} a_{n+k})$. Substituting (13) into (12) will yield

$$\text{PMERP} = \frac{\max\left(\sum_{n=0}^{N-1}\left|w_n b_n a_n\right|^2 + 2\text{Re}\left\{\sum_{k=1}^{N-1} m_k \exp\left(j2\pi k\Delta f t\right)\right\}\right)}{(1/t_b)\int_0^{t_b}\left(\sum_{n=0}^{N-1}\left|w_n b_n a_n\right|^2\right)dt}. \tag{14}$$

Equation (14) shows that the PMERP is determined by the self-correlation function of sequence $w_n b_n a_n$, where b_n is the random communication data, $w_n = A_n \varphi_n$ is the complex weight, and a_n is the circular shift. A closer inspection reveals that the circular shift a_n has no effect on the self-correlation function m_k; in other words, a_n does not change the PMERP of RadCom waveform. Therefore only w_n and b_n can be utilized to control the PMERP. Typically, the amplitude A_n is set as window functions including rectangular, Hamming, and Blackman window, and phase φ_n is set as Newman, Schroeder, or Narahashi-Nojima phase. For the random communication data b_n, phase-encoding technology is always adopted to reduce the PMERP of RadCom waveform.

4.2. Theoretical Analysis of PSLR. Radar ambiguity function is an effective tool for radar waveform analysis and design. Here, we first give the derivation procedure of ambiguity function of the proposed RadCom waveform and then combine the ambiguity functions to analyze the designed waveform.

The RadCom waveform represented in (4) can be rewritten as

$$S_{RC}(t) = \sum_{n=0}^{N-1} w_n u_n(t) \exp\left(j2\pi f_n t\right), \quad 0 \le n < N, \tag{15}$$

where $u_n(t) = \sum_{m=1}^{M} d_{m,n} u[t-(m-1)t_b]$ and $d_{m,n} = b_{m,n} a_{m,n}$. Then the ambiguity function of RadCom waveform can be defined as

$$\begin{aligned}\chi(\tau, f_d) &= \int_{-\infty}^{+\infty} S_{RC}(t)\, S_{RC}{}^{*}(t+\tau) \exp\left(j2\pi f_d t\right) dt \\ &= \sum_{n=0}^{N-1}\sum_{l=0}^{N-1} w_n w_l{}^{*} \int_{-\infty}^{+\infty} u_n(t)\, u_l{}^{*}(t+\tau) \\ &\cdot \exp\left(j2\pi\left[(n-l)\Delta f + f_d\right] t\right) \exp\left(-j2\pi l \Delta f \tau\right) \\ &= \chi_{\text{Auto}}(\tau, f_d) + \chi_{\text{Cross}}(\tau, (n-l)\Delta f + f_d),\end{aligned} \tag{16}$$

$$\chi_{\text{Auto}}(\tau, f_d) = \sum_{n=0}^{N-1} w_n{}^{2} \chi_n(\tau, f_d) \exp\left(-j2\pi n \Delta f \tau\right), \tag{17}$$

$$\begin{aligned}\chi_{\text{Cross}}(\tau, f_d) &= \sum_{n=0}^{N-1}\sum_{l=0,l\ne n}^{N-1} w_n w_l{}^{*} \chi_{n,l}(\tau, f_d) \\ &\cdot \exp\left(-j2\pi l \Delta f \tau\right),\end{aligned} \tag{18}$$

where $\chi_{\text{Auto}}(\tau, f_d)$, obtained by setting $n = l$, is the main part of the ambiguity function, $\chi_{\text{Cross}}(\tau, f_d)$ achieved when $n \ne l$ is the mutual interference, $\chi_n(\tau, f_d)$ is the ambiguity function of $u_n(t)$, and $\chi_{n,l}(\tau, f_d)$ is the cross ambiguity function of $u_n(t)$ and $u_l(t)$. Notice that $u_n(t)$ is a phase-encoding sequence with a length M and the duration of a subpulse is t_b. Then the ambiguity function of $u_n(t)$ is given as

$$\chi_n(\tau, f_d) = \sum_{k=-(M-1)}^{M-1} \chi_1(\tau - kt_b, f_d) \cdot \chi_2(kt_b, f_d), \tag{19}$$

where $\chi_1(\tau - kt_b, f_d)$ is the ambiguity function of a subpulse $u(t)$ and $\chi_2(kt_b, f_d)$ is the ambiguity function of phase-encoding sequence and they are defined as

$$\begin{aligned}&\chi_1(\tau, f_d) \\ &= \begin{cases} \dfrac{\sin\left[\pi f_d\left(t_b - |\tau|\right)\right]}{\pi f_d} \exp\left[j\pi f_d\left(t_b - \tau\right)\right], & |\tau| \le t_b, \\ 0, & |\tau| > t_b, \end{cases} \\ &\chi_2(kt_b, f_d) = \sum_{m=0}^{M-1-|k|} d_{m,n} d^{*}{}_{m+|k|,n} \exp\left(j2\pi f_d k t_b\right).\end{aligned} \tag{20}$$

Similar to $\chi_n(\tau, f_d)$, $\chi_{n,l}(\tau, f_d)$ is defined as

$$\begin{aligned}\chi_{n,l}(\tau, f_d) &= \sum_{k=-(M-1)}^{M-1} \chi_1(\tau - kt_b, f_d) \cdot \chi_3(kt_b, f_d), \\ \chi_3(kt_b, f_d) &= \sum_{m=0}^{M-1-|k|} d_{m,n} d^{*}{}_{m+|k|,l} \exp\left(j2\pi f_d k t_b\right).\end{aligned} \tag{21}$$

Substituting (19)–(21) into (16) yields

$$\begin{aligned}\chi(\tau, f_d) = \chi_{\text{Auto}}(\tau, f_d) + \chi_{\text{Cross}}(\tau, (n-l)\Delta f + f_d) &= \sum_{n=0}^{N-1}\sum_{k=-(M-1)}^{M-1}\sum_{m=0}^{M-1-|k|} |w_n|^2 d_{m,n} d^{*}{}_{m+|k|,n} \frac{\sin\left[\pi f_d\left(t_b - |\tau - kt_b|\right)\right]}{\pi f_d} \\ \cdot \exp\left[j\pi f_d\left(t_b - \tau + kt_b\right) - j2\pi n \Delta f \tau\right] &+ \sum_{n=0}^{N-1}\sum_{l=0,l\ne n}^{N-1}\sum_{k=-(M-1)}^{M-1}\sum_{m=0}^{M-1-|k|} w_n w_l{}^{*} d_{m,n} d^{*}{}_{m+|k|,l} \frac{\sin\left[\pi f_d\left(t_b - |\tau - kt_b|\right)\right]}{\pi\left[(n-l)\Delta f + f_d\right]} \\ \cdot \exp\left[j\pi\left((n-l)\Delta f + f_d\right)\left(t_b - \tau + kt_b\right) - j2\pi l \Delta f \tau\right].\end{aligned} \tag{22}$$

Notice that $(\sin[\pi f_d(t_b - |\tau - kt_b|)])/\pi[(n-l)\Delta f + f_d])|_{f_d=0, n\ne l} = 0$; thus the autocorrelation function can be simplified as

$$\begin{aligned}\chi(\tau, 0) = \sum_{n=0}^{N-1}\sum_{k=-(M-1)}^{M-1}\sum_{m=0}^{M-1-|k|} &|w_n|^2 \left(b_{m,n} a_{m,n}\right) \\ &\cdot \left(b_{m,n} a_{m,n}\right)^{*}{}_{m+|k|,n} \cdot \left(t_b - |\tau - kt_b|\right) \\ &\cdot \exp\left(-j2\pi n \Delta f \tau\right).\end{aligned} \tag{23}$$

From (14) and (23), we can see that the PMERP and autocorrelation of RadCom waveform are related to complex weight w_n, communication data b_n, and time-domain circular shift $a_{m,n}$. For a radar system, the complex weight is often set as window functions with initial phase to reduce the PMERP or improve the PSLR of system. However, in a RadCom system, the randomness of communication data will destroy the integrity of the window functions and further affect the PMERP and PSLR of system. To address these issues, in this paper, communication data is encoded by Gray code to reduce the PMERP of RadCom waveform to 3 dB and complex weight is set as rectangle window without initial phase to maintain the integrity of the Gray sequence. As was discussed earlier, time-domain circular shifted $a_{m,n}$ has no effect on the PMERP but can be used to suppress the SLL of RadCom waveform. Thus, a suitable choice of $(a_1, a_2, \ldots, a_M)$ can be selected to simultaneously achieve a higher PSLR and lower PMERP. For the communication function of a RadCom waveform, data rate and BER are two important parameters. In this paper, the communication data depends on the number of subcarriers of RadCom waveform and BER only relates to the modulation mode and SNR. For a given RadCom waveform, its communication performance is obvious; thus the communication performance discussion of RadCom waveform is ignored in this paper.

5. Simulation Results and Analysis

In the simulation experiments, we first discuss the parameter settings of OFDM based RadCom waveform and then verify the PMERP reduction and SLL suppression performance of the designed RadCom waveform.

In this paper, our proposed RadCom waveform is based on the 5.8 GHz ISM band. From both the communications and the radar perspective, most of the parameterization criteria are in fact identical, since they are related to physical properties of the channel. The limiting properties of the channel are mainly the Doppler spread and the maximum multipath delay. Assuming the maximum relative velocity is 200 km/s, then the maximum Doppler shift of the reflected signal is $f_D = 2.1$ kHz. According to typical OFDM system design rules, the subcarrier spacing must be satisfied with $\Delta f > 10 f_D$ to ensure the orthogonality of the subcarriers [25]. For the radar application, there is a direct coupling between transmitting and receiving antenna; hence the cyclic prefix duration must be longer than the roundtrip travel time between the radar transmitter and the most distant target. Here we assume that the radar receiver sensitivity is −65 dBm, RCS is 1 m^2, and the EIRP power limitation of the 5.8 GHz ISM regulation is 33 dBm. Thus the maximum detectable range is 1200 m, which results in a minimum cyclic prefix duration $T_G > 8$ us. The complete set of OFDM based RadCom waveform parameters is listed in Table 1. One point to note is that the bandwidth can be adjusted conveniently according to the radar detection requirements and the bandwidth shown in Table 1 is just an example.

Table 1: Parameters of the RadCom waveform.

Parameters	Value
Center frequency (f_c)	5.8 GHz
Baseband bandwidth (B)	32 MHz
Numbers of subcarriers (N_c)	128
Frequency interval (Δf)	250 kHz
Radar range resolution	4.69 m
Cyclic prefix duration (T_G)	10 μs
Element OFDM symbol duration (T)	4 μs
Total OFDM symbol duration (T_{OFDM})	14 μs
Number of OFDM symbols (M)	16
Processing gain (G_p)	33.1 dB

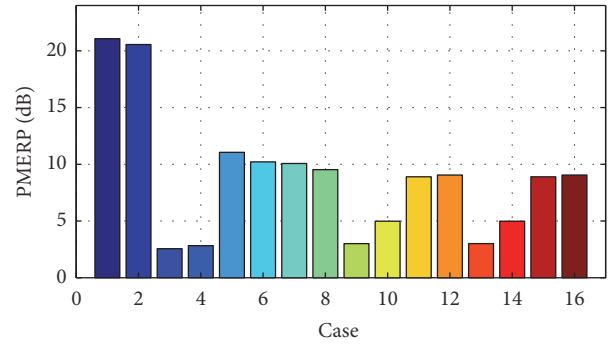

Figure 4: PMERP simulation results in cases (1–16).

5.1. PMERP Performance of RadCom Waveform. In this section, the impacts of w_n, b_n, and a_n on the proposed RadCom waveform are validated in 16 cases. The amplitude and phase of frequency weight are set as rectangular window and zero value in case (1), Hanning window and zero value in case (2), rectangular window and Newman in case (3), and Hanning window and Newman in case (4), respectively. In cases (1–4), the value of communication data sequence is set as one. On the contrary, in cases (5–8), the communication data sequences are random and the frequency weights are set the same as those in cases (1–4). In cases (9–12), the frequency weights are set the same as those in cases (5–8). But the difference is that the communication data in cases (9–12) are encoded with Gray code. Cases (13–16) are a cyclic shift version of that in cases (9–12). The PMERP simulation results in cases (1–16) with 4 times oversampling are shown in Figure 4.

In cases (1–8), it can be seen that when the value of communication data is set as one, a Newman initial phase will greatly reduce the PMERP of RadCom waveform. However, when the communication data is random, the performance of Newman initial phase will decline. The reason is that the complex weight sequences w_n arranged according to certain rules cannot eliminate the uncertain nature of communication data. Cases (9–12) show that when the communication data is encoded by Gray code, the rectangle window with zero initial phase has the lowest PMERP, while when the Hanning window with or without Newman initial phase is adopted, the PMERP will increase. That is because the

Table 2: PMEPR and SLL of RadCom waveform in three different situations.

RCI waveform	Method 1/128 MHz		Method 2/128 MHz	
	SLL (dB)	PMERP (dB)	SLL (dB)	PMERP (dB)
Circular shift sequence	−26.8279	3.0102	−18.9341	3.0002
M (Gray code + M sequence)	−24.5142	7.6624	−13.0208	6.9346
Chaos (Gray code + chaos sequence)	−24.1496	8.9534	−14.3595	8.1051
M (window + M sequence)	−23.8604	8.0175	−8.8352	7.2843
Chaos (window + chaos sequence)	−22.9803	9.0233	−7.5055	8.1510

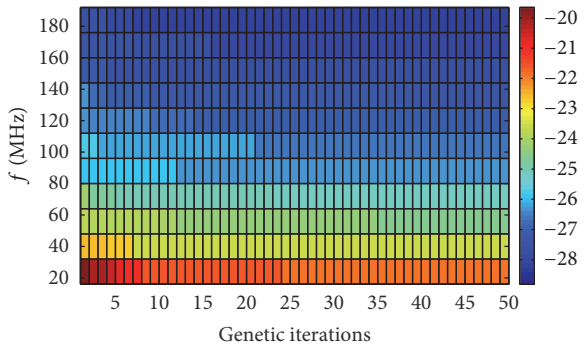

Figure 5: PSLR of RadCom waveform versus the genetic iterations.

integrality of Gray code is destroyed by Hanning window or Newman phase. For a RadCom waveform, both of b_n and w_n seemingly can be adjusted to reduce the PMERP, but in fact the communication data and complex weight interfered with each other. Therefore to achieve a lower PMERP, setting the complex weight as a constant and using Gray code to encode the communication data will be a reasonable choice. Cases (13–16) demonstrate that the circular shift a_n has no effect on the PMERP of RadCom waveform. However, the circular shift plays an important role in the SLL suppression of RadCom waveform. This means that we can improve the PSLR of RadCom waveform and simultaneously keep a lower PMERP by the suitable choice of $(a_1, a_2, \ldots, a_M)$.

5.2. Radar Performance of RadCom Waveform. We compare the radar performances of RadCom waveform in three different situations, where $a_{m,n}$ are designed as direct spread spectrum sequence [15], chaos-based phase code sequence [17], and cyclic shift sequence, respectively. In view of the various requirements of different radar detection tasks, the bandwidth of RadCom waveform varying from 16 MHz to 200 MHz is generated by method 1 or method 2. In the simulation experiments, the direct spread spectrum sequence is generated by m-sequence and chaos-based sequence is generated by logistic map with initial $x_0 = 0$, $\lambda = 0.5$. The optimal circular shift sequence is achieved by genetic algorithm where the number of individuals in the population is set as 20 and the max number of genetic iterations is 50. To verify the effectiveness of genetic algorithm, the SLLs of RadCom waveform with different bandwidths and iteration numbers are shown in Figure 5.

From Figure 5, it can be seen that the PSLR of RadCom waveform is improved with the increasing of genetic iterations, which demonstrates the effectiveness of GA method. In addition, it is not difficult to find that the SLL suppression achieves a better result with the bandwidth increasing. A more detailed result about this issue is shown in Figure 6.

Figure 6(a) shows that the PSLR of RadCom waveform with a wide bandwidth performs better than that with a narrow bandwidth in method 1. The reason may be that in method 1 the RadCom bandwidth is enlarged by adding the number of subcarriers, which results in a long RadCom sequence, and a long sequence often offers a better autocorrelation performance. From the overall view of Figure 6, we can also see that the radar performance of proposed method is better than that of other methods. One point to be clear is that in our approach the PMERP is reduced to 3 dB, while in other methods the PMERP is larger than 3 dB. In other words, a lower PMERP and SLL can be simultaneously realized by our method. Contrary to Figure 6(a), Figure 6(b) illustrates that the SLL of RadCom waveform is not reduced with the bandwidth increasing in method 2. That is because, even with an increase on the bandwidth of RadCom, the length of sequence remains the same. Thus the autocorrelation performance of the RadCom waveform is not improved. From Figure 6(b), it also can be seen that the PSLR performance of RadCom without window function is superior to that with window function. The reason is that the integrity of the m-sequence or chaos-based sequence is destroyed by the window function, which degrades the radar performance of RadCom waveform. Different from the methods of m-sequence and chaos-based sequence, in our method there is no need to use the window functions to reduce the PMERP and the integrity of circular shift sequence will not be destroyed. Therefore, our method has a better PMERP performance and the SLL of RadCom waveform can be reduced nearly by 5 dB compared with other methods. To further verify the effectiveness of the proposed method, the detailed results of PMERP and SLL with three different phase sequences $a_{m,n}$ designing at a point $B = 128$ MHz are shown in Table 2.

Table 2 shows that m-sequence or chaos-based sequence cannot achieve a lower PMERP and SLL simultaneously. The reason is that when Gray code is adopted, the integrity of Gray code is destroyed by m-sequence or chaos-sequence, while when window function is adopted, the window function and sequence interact with each other, which destroys the integrity of them. In this paper, the PMERP of RadCom waveform is reduced by Gray code instead of window function. Therefore, the combination of Gray code technology and

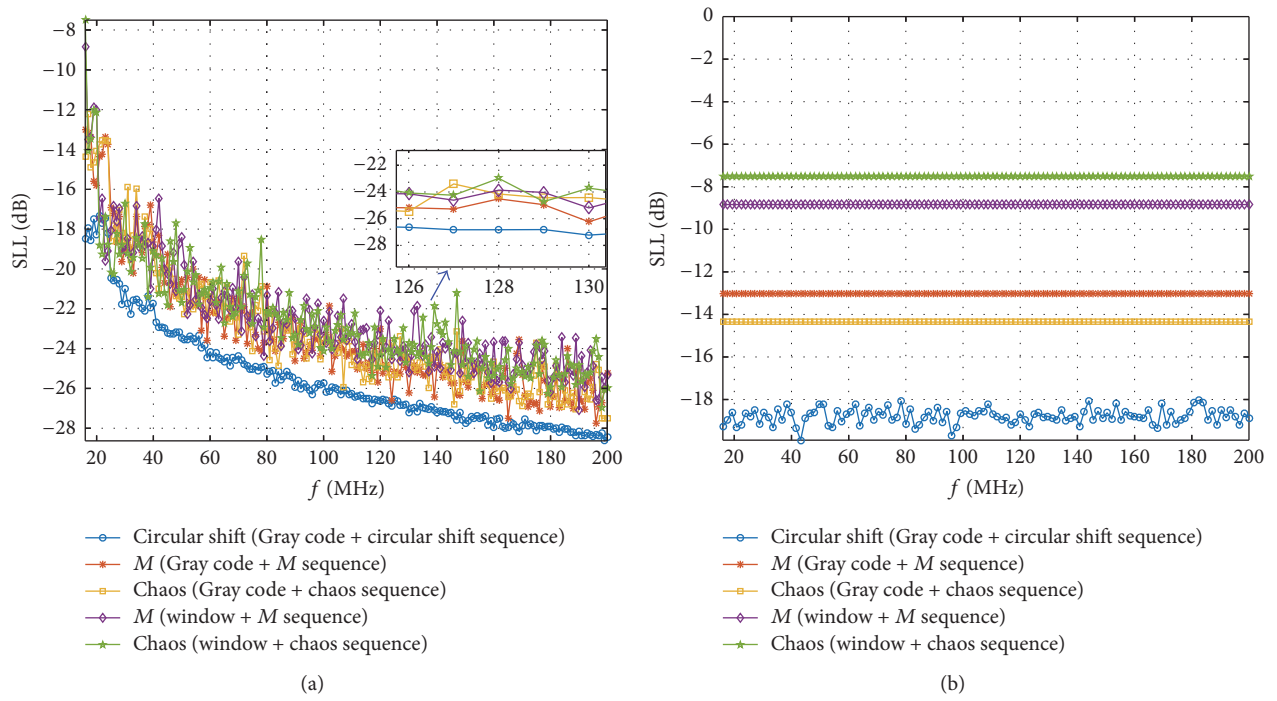

Figure 6: SLL of RadCom waveform with different phase sequences design. (a) Expanding the bandwidth of RadCom waveform by method 1; (b) expanding the bandwidth of RadCom waveform by method 2.

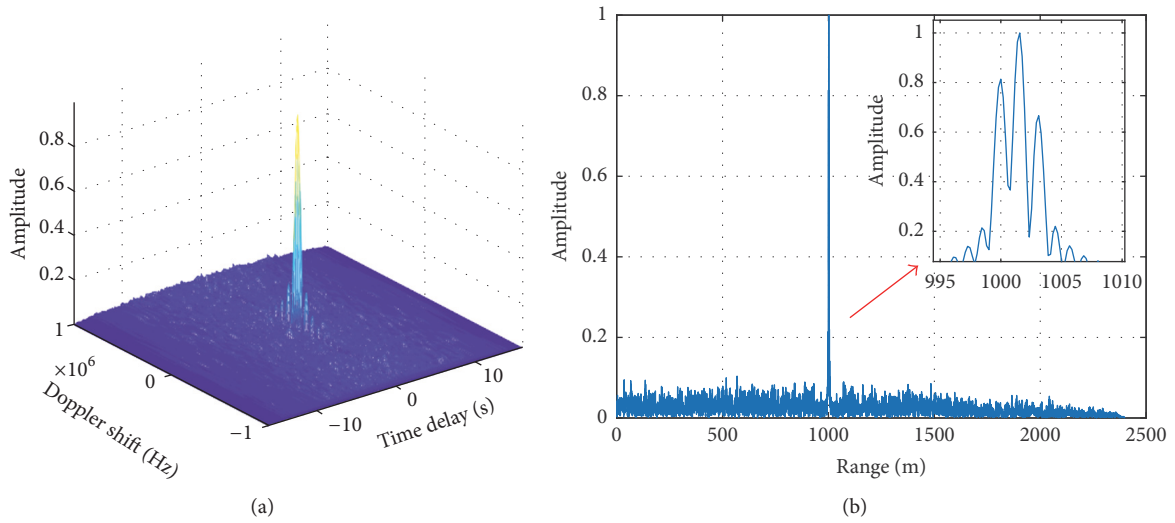

Figure 7: Fuzzy function and HRRP of RadCom waveform. (a) Fuzzy function; (b) one-dimension HRRP.

circular shift method can be utilized to simultaneously reduce the PMERP and SLL of RadCom waveform.

Next, the fuzzy function and multitarget detection capability of the proposed RadCom waveform are validated. In the simulation experiment, we assume that there are three static targets and the reflection coefficient and distance of them to radar are 0.8, 1000 m, 1.0, 1001.5 m, and 0.6, 1003 m, respectively. Besides, in the experiments, the SNR is set as 5 dB and bandwidth equals 128 MHz. The simulation results are shown in Figure 7.

Figure 7(a) shows that our designed RadCom waveform has a good thumbtack type ambiguity function, which means that the range and Doppler are not coupled and can be processed separately. Figure 7(b) denotes that the three targets with a mutual distance of 1.5 meters can be detected by the proposed RadCom waveform and the peaks of HRRP of three

targets are consistent with the given reflection coefficients. In a word, Figure 7 shows that radar function can be well performed by our proposed RadCom waveform.

6. Conclusion

PMERP and PSLR are two major problems in the OFDM based RadCom waveform design, which are analyzed and solved perfectly in this paper. For the PMERP problem, the influences of frequency weight and random communication data are discussed. Based on the analysis results of PMERP, a Gray code technique is adopted to reduce the PMERP to 3 dB. Similar to the PMERP problem, based on the analysis results of PSLR, we propose a suitable cyclic shift sequence to improve the SLL suppression. To validate the effectiveness of designed RadCom waveform in terms of PSLR, we carry on contrast experiments with m-sequence and chaos-based sequence methods. The simulation results show that the SLL of RadCom waveform can be further reduced by more than 2 dB in the first bandwidth increasing method and 5 dB in the second bandwidth increasing method compared with the other methods. This means that our proposed RadCom waveform can simultaneously achieve a lower PMERP and higher PSLR. In addition, our designed RadCom waveform has a thumbtack type fuzzy function and shows the good ability to detect multiple targets.

Conflicts of Interest

The authors declare that there are no conflicts of interest regarding the publication of this paper.

References

[1] D. W. Bliss, "Cooperative radar and communications signaling: the estimation and information theory odd couple," in *Proceedings of the 2014 IEEE Radar Conference, RadarCon 2014*, pp. 50–55, Cincinnatim, Ohio, USA, 2014.

[2] R. A. Romero and K. D. Shepherd, "Friendly spectrally shaped radar waveform with legacy communication systems for shared access and spectrum management," *IEEE Access*, vol. 3, pp. 1541–1554, 2015.

[3] D. Ciuonzo, A. De Maio, G. Foglia, and M. Piezzo, "Intrapulse radar-embedded communications via multiobjective optimization," *IEEE Transactions on Aerospace and Electronic Systems*, vol. 51, no. 4, pp. 2960–2974, 2015.

[4] C. Mai, J. Sun, R. Zhou, and G. Wang, "Sparse frequency waveform design for radar-embedded communication," *Mathematical Problems in Engineering*, vol. 2016, Article ID 7270301, 2016.

[5] A. Hassanien, M. G. Amin, Y. D. Zhang, and F. Ahmad, "Dual-function radar-communications: information embedding using sidelobe control and waveform diversity," *IEEE Transactions on Signal Processing*, vol. 64, no. 8, pp. 2168–2181, 2016.

[6] A. Hassanien, M. G. Amin, Y. D. Zhang, and F. Ahmad, "Dual-function radar-communications using phase-rotational invariance," in *Proceedings of the 23rd European Signal Processing Conference, EUSIPCO 2015*, pp. 1346–1350, 2015.

[7] C. Sturm, T. Zwick, and W. Wiesbeck, "An OFDM system concept for joint radar and communications operations," in *Proceedings of the VTC Spring 2009 - IEEE 69th Vehicular Technology Conference*, 2009.

[8] D. Garmatyuk, J. Schuerger, K. Kauffman, and S. Spalding, "Wideband OFDM system for radar and communications," in *Proceedings of the 2009 IEEE Radar Conference, RADAR 2009*, pp. 1–6, 2009.

[9] S. D. Blunt and C. R. Biggs, "Practical considerations for intra-pulse radar-embedded communications," in *Proceedings of the International Waveform Diversity and Design Conference (WDD '09)*, pp. 244–248, Kissimmee, Fla, USA, February 2009.

[10] L. Han and K. Wu, "Multifunctional transceiver for future intelligent transportation systems," *IEEE Transactions on Microwave Theory and Techniques*, vol. 59, no. 7, pp. 1879–1892, 2011.

[11] S. Lindenmeier, K. Boehm, and J. F. Luy, "A wireless data link for mobile applications," *IEEE Microwave and Wireless Components Letters*, vol. 13, no. 8, pp. 326–328, 2003.

[12] Z. Lin and P. Wei, "Pulse amplitude modulation direct sequence ultra wideband sharing signal for communication and radar systems," in *Proceedings of the International Symposium on Antennas, Propagation & Em Theory*, p. 1, 2006.

[13] M. Bocquet, "A multifunctional 60-GHz system for automotive applications with communication and positioning abilities based on time reversal," in *Proceedings of the Radar Conference (EuRAD)*, pp. 61–64, Paris, French, 2010.

[14] K. Mizui, M. Uchida, and M. Nakagawa, "Vehicle-vehicle communication and ranging system using spread spectrum technique," in *Proceedings of the 43rd IEEE Vehicular Technology Conference*, pp. 335–338, 1993.

[15] L. Hu, Z. Du, and G. Xue, "Radar-communication integration based on OFDM signal," in *Proceedings of the 2014 IEEE International Conference on Signal Processing, Communications and Computing, ICSPCC 2014*, pp. 442–445, 2014.

[16] D. Garmatyuk, "Radar and data communication fusion with UWB-OFDM software-defined system," in *Proceedings of the 2009 IEEE International Conference on Ultra-Wideband, ICUWB 2009*, pp. 454–458, 2009.

[17] J. Zhao, K. Huo, and X. Li, "A chaos-based phase-coded OFDM signal for joint radar-communication systems," in *Proceedings of the 2014 12th IEEE International Conference on Signal Processing, ICSP 2014*, pp. 1997–2002, 2014.

[18] N. Levanon, "Multifrequency complementary phase-coded radar signal," *IEE Proceedings: Radar, Sonar and Navigation*, vol. 147, no. 6, pp. 276–284, 2000.

[19] S. C.-H. Huang, H.-C. Wu, S. Chang, and X. Liu, "Novel sequence design for low-PMEPR and high-code-rate OFDM systems," *IEEE Transactions on Communications*, vol. 58, no. 2, pp. 405–410, 2010.

[20] E. Mozeson and N. Levanon, "Multicarrier radar signals with low peak-to-mean envelope power ratio," *IEE Proceedings: Radar, Sonar and Navigation*, vol. 150, no. 2, pp. 71–77, 2003.

[21] R. F. Tigrek, "A method for measuring the radial velocity of a target with a Doppler radar," 2009, European Patent.

[22] R. F. Tigrek, W. J. A. De Heij, and P. Van Genderen, "Multi-carrier radar waveform schemes for range and doppler processing," in *Proceedings of the 2009 IEEE Radar Conference, RADAR 2009*, 2009.

[23] A. G. Armada and M. Calvo, "Phase noise and sub-carrier spacing effects on the performance of an OFDM communication system," *IEEE Communications Letters*, vol. 2, no. 1, pp. 11–13, 1998.

[24] T. Huang and T. Zhao, "Low PMEPR OFDM radar waveform design using the iterative least squares algorithm," *IEEE Signal Processing Letters*, vol. 22, no. 11, pp. 1975–1979, 2015.

[25] M. Engels, "Wireless OFDM systems: how to make them work?" *IEEE Communications Magazine*, vol. 41, no. 2, pp. 16–18, 2003.